



UNIVERSITY OF NIŠ
The scientific journal FACTA UNIVERSITATIS
Series: **Physics, Chemistry and Technology** Vol. 2, No 1, 1999 pp. 47 - 61
Editor of series: Momčilo Pejović, e-mail: pejovic@elfak.ni.ac.yu
Address: Univerzitetski trg 2, 18000 Niš, YU
Tel: +381 18 547-095, Fax: +381 18 547-950

ISOTHERMAL AND ISOCHRONAL ANNEALING OF GAMMA-RAY IRRADIATED n-CHANNEL POWER VDMOS TRANSISTORS

UDC 538.9+613.648.4

Goran S. Ristić, Momčilo M. Pejović, Aleksandar B. Jakšić

Faculty of Electronic Engineering, University of Niš, Beogradska 14, 18000 Niš
E-mail: goranristic@elfak.ni.ac.yu

Abstract. *The behaviour of densities of the oxide trapped charge and the interface traps in gamma-ray irradiated n-channel power VDMOS transistors during isothermal and isochronal annealing has been investigated. The experimental results have revealed the existence of latent interface trap buildup (LITB) process. By using of numerical modeling, based on the H-W model, the LITB process during isothermal annealing has been successfully simulated. The interface trap densities have been determined by both the midgap and the charge pumping methods, and results have shown good qualitative agreement between these two methods.*

Key words: *interface traps, oxide trapped charge, irradiation, annealing, MOS transistors*

1. INTRODUCTION

As the consequence of the influence of ionizing radiation on metal-oxide-semiconductor (MOS) transistors, the positive trapped charge in the gate oxide and the interface traps at Si/SiO₂ interface are formed [1]. To understand the behaviour of these defects is very important, since they can degrade the electrical performance of MOS transistors: threshold voltage, transconductance, leakage current and breakdown voltage. Also, the investigation of the radiation defects is very important for the ionizing radiation dosimetry, which can be based on p-channel MOS (pMOS) dosimetric transistors [2-7].

The particular attention should be given to the annealing of irradiated transistors, because of possible existence of latent interface trap buildup (LITB) process [8-10]. LITB process is defined as a sudden rapid increase in interface traps during postirradiation annealing after apparent saturation of the interface trap density immediately following

irradiation [8,9]. Compared to the time scale of normal (conventional) interface trap buildup, i.e. interface trap buildup that occurs during and immediately after irradiation, the time scale of LITB process is much longer. The LITB process is not yet completely understood, although recent investigations [11-14] of hydrogen cracking in the gate oxide of irradiated MOS transistors have helped understanding this process.

Our recent investigations [15-19] have shown the existence of the LITB process in gamma-ray irradiated n-channel power vertical double-diffused metal-oxide-semiconductor (VDMOS) transistors during annealing at relatively lower temperatures (room-temperature, 55 and 140 °C). These experimental results have been explained by the hydrogen-water (H-W) model [15,16]. The aim of this paper is investigation of the behaviours of oxide trapped charge density and interface trap density during annealing at higher temperature values. Also, by performing the isochronal annealing experiment, the validity of the H-W model is further checked.

2. EXPERIMENTAL DETAILS

The devices used in these experiments were commercial n-channel power VDMOS transistors EFP8N15, manufactured by Ei-Microelectronics, Ni{ (the transistor consists of 5174 hexagonal cells). The maximum voltage of these devices is 150 V, and maximum current is 8 A. The effective channel length is 2.6 μm , and the channel width of a single cell is 62.4 μm (for more detailed description of the hexagonal cell see Refs. [19,20]). The starting material was 400 μm thick n-type Si wafers with (100) orientation, on which the n-epi layer of about 14 μm was grown. After implantation of the p⁺-body region, the gate oxide with nominal thickness of 100 nm was grown in dry oxygen at 1100 °C, and annealed in nitrogen at 1100 °C for 20 min. There followed the deposition of 800 nm thick poly-Si gate, implantation of the p-channel and n⁺-source regions, and deposition of 1 μm thick CVD oxide. After metalization and post-metalization anneal at 550 °C in nitrogen, devices were mounted in standard plastic TO-220 packages.

The transistors were irradiated at room temperature using a ⁶⁰Co source at a dose rate of 0.01 Gy(Si)/s, to the total dose of 150 Gy (Si). The irradiation was performed in the Metrology Laboratory of the Institute for nuclear science 'Vin-a', Vin-a-Belgrade. During irradiation, the gate bias (V_G) was kept at 10 V. After irradiation, the transistors were annealed in air at different temperatures (140, 200, 250 and 290 V) with $V_G = 10$ and -10 V, using the Heraeus HEP2 system of temperature chambers with high temperature stability. During both the irradiation and annealing, the source and drain terminals were grounded.

Transistor subthreshold and transfer characteristics in saturation were measured at room-temperature. Equipment used for electrical characterisation consisted of a HP 8116A function generator and Keithley 237 Source-Measure-Unit (SMU), both controlled by a PC (Fig. 1). Namely, using HP 8116A the DC voltage was applied to the transistor gate (G), and the drain (D) was biased ($V_D = 10$ V) and drain-source current (I_{DS}) measured by the Keithley 237 SMU (the source was grounded). The threshold voltage was determined as the intersection between V_G -axis and the extrapolated linear region of

the $(I_{DS})^{1/2}$ - V_G curve.¹ The midgap-subthreshold (MG) method [21] was used to determine the areal densities of positive gate oxide trapped charge (ΔN_{ot} [cm^{-2}]) and interface traps (ΔN_{it} [cm^{-2}]).

The charge-pumping (CP) method [22,23,20] for determination of ΔN_{it} was also used. Using HP 8116A function generator, the triangular pulses with the frequency of $f = 100$ kHz, duty cycle 50 % and amplitude of $\Delta V_A = 3$ V were applied to the transistor gate, while the source was grounded. The CP current (I_{cp}) was measured at drain terminals by the Keithley 237 SMU. The measurement system also contains the PC with interface card under control of a Turbo Pascal program (Fig. 2).

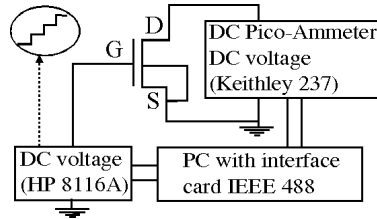


Fig. 1. Block diagram of the experimental set-up for MG measurements.

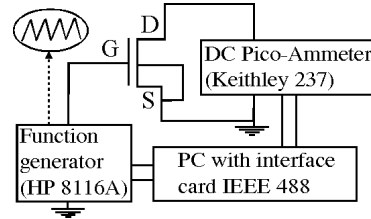
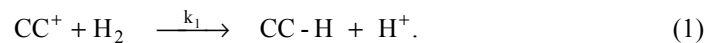


Fig. 2. Block diagram of the experimental set-up for CP measurements.

3. THE HYDROGEN-WATER (H-W) MODEL

In our previous papers [15-19], it has been shown that the H-W model can describe the LITB process during annealing of irradiated MOS transistors. In the following text, the most important characteristics of the H-W model will be briefly described. The H-W model starts of the fact that a small concentration of H^+ ions exists at the Si/SiO₂ interface² after long annealing time. One of the possible sources of H^+ ions are H₂ molecules, which arrive from the adjacent structures (CVD oxide and poly-Si gate) to the gate oxide. Namely, H₂ molecules are released in CVD oxide or/and poly-Si gate, and slowly diffuse towards the interface (see the structure of used transistors [19]). It has been confirmed that the diffusion constants of hydrogen are decreased in poly-Si gate [24] and irradiated thermal oxide [25]. In the vicinity of the interface, these molecules are cracked at positively charged centers CC^+ in the oxide, forming hydrogen ions [11]:



The H^+ ions, formed in reaction (1), drift towards the interface under positive electric field in the oxide.³

Another possibility is that H^+ ions, formed during irradiation, are captured by oxygen vacancies and represent gate oxide trapped charge [10,26]. During annealing they are liberated and drift towards the interface. However, the contribution of captured hydrogen

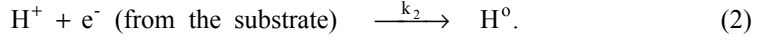
¹ The least square method performed by MATLAB program package was used.

² In following text "interface".

³ It is supposed that the positive bias is applied to the gate.

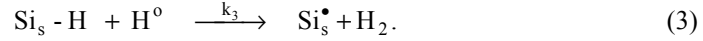
ions to ΔN_{ot} should be relatively small, since it has been shown that almost all of oxide trapped charge are E' centers [27,28]. Fleetwood et al. [10] have supposed that captured H^+ ions can make about 10-20 % of net oxide charge density. Also, H_2O molecules can be responsible for the beginning of the LITB process [18].

When H^+ ion arrives at the interface, it picks up an electron from the substrate [29]:



Liberated highly reactive H^0 atom may react without an energy barrier [30,31] in one of the following manners:

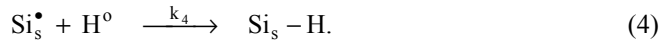
- (i) The creation of the interface trap Si_s^\bullet ,⁴ when H^0 reacts with an interface trap precursor Si_s-H [29]:



The P_{b0} and P_{b1} centers, which exist at (100) interface, represent interface traps [32,33]. The P_{b0} defect has the structure: $\equiv Si_{s0}^\bullet$,⁵ while the structure of the P_{b1} defect, here denoted as $\equiv Si_{s1}^\bullet$, is not yet known (remaining three bonds of $\equiv Si_{s1}^\bullet$ defect can be bonded to various species). It can be proposed that either the $\equiv Si_{s0}-H$ defect, precursor of the P_{b0} center, or some hypothetical $\equiv Si_{s1}-H$ defect, precursor of the P_{b1} center, are responsible for interface trap increase during annealing. In the following text, since remaining three bonds of P_{b0} and P_{b1} defects are not significant, these centers will be denoted as Si_s^\bullet , and their precursors as Si_s-H .

It should be noted that Kim and Lenahan [28] have shown that the P_{b0} centers are largely responsible for the behaviour of interface traps and that the density of radiation-induced P_{b1} can be neglected. Oppositely, the results of some investigations [34,31] have shown that other center or centers probably exist at the interface and act as interface traps. However, since structure and behaviour of these centers haven't been given, they will not be considered in this analysis.

- (ii) The passivation of the interface trap, when H^0 reacts with previously formed (fabrication process-, radiation- or annealing-induced) interface trap [30,35]:



- (iii) Dimerization of hydrogen, when H^0 reacts with another H^0 also existing near the interface [36,37]:



It should be noted that the reaction (3) is the most probable at the start of the LITB process [18].

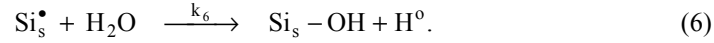
The H_2 molecules formed in reaction (3) diffuse towards the bulk of the gate oxide and can be cracked at CC^+ centers (reaction (1)). So, the reaction (1) represents the

⁴ The point denotes unpaired electron, i.e. "uncoupled spin".

⁵ $\equiv Si_{s0}^\bullet$ defect denotes silicon atom at the oxide-silicon interface back bonded to three silicon atoms from substrate and is elsewhere represented as $Si_3 \equiv Si_{s0}^\bullet$.

continuous source of H^+ ions during long time annealing. These ions drift towards the interface to form interface traps. It means that only a small initial concentration of H^+ ions is needed for the start of LITB process. The remaining H^+ ions necessary for formation of maximum ΔN_{it} ($\Delta N_{it,max}$) are produced during the LITB process itself in reaction (1) through the repetitive reaction sequence (1) \Rightarrow (2) \Rightarrow (3) \Rightarrow (1) or (1) \Rightarrow (5) \Rightarrow (1). Also, the reaction (1) is an additional mechanism for neutralisation of oxide trapped charge, as well as the explanation for the dependence of ΔN_{it} increase rate on temperature (see the following text).

Reactions (1)-(5) can explain the interface trap creation. However, for the explanation of experimentally observed decrease of ΔN_{it} at very late annealing times, it is necessary to include at least one additional reaction. According to the H-W model, interface trap passivation process can be explained by the following reaction of H_2O molecules at the interface [18]:



It would be expected [18] that the H_2O concentration will first increase, up to its maximum value, and then slowly decrease. One possible description of this would be: $[H_2O] = k_7 t \exp(-a t^n)$, where k_7 , a and n are constants, and t is annealing time.

4. EXPERIMENTAL RESULTS AND DISCUSSION

Figure 3 shows the changes in ΔN_{ot} and ΔN_{it} during annealing at various temperatures with $V_G = 10$ V. As it can be seen, these changes very much depend on the annealing temperature. The main characteristics of these experimental results are: 1) very great values of $\Delta N_{it,max}$ created during the LITB process, 2) the explicit dependence of creation rate of interface traps on temperature - ΔN_{it} increase rate rises with temperature (note the log-scale for time axis), and 3) the decrease of ΔN_{it} after long annealing times. Also, the correlation between the increase of ΔN_{it} and the decrease of ΔN_{ot} is observed at all investigated temperatures.

In previous papers [17,18], the numerical simulation has shown that hydrogen ion transport H^+ model [29,38,39] cannot explain this behaviour. It has been supposed [17] that the H^+ model contains reactions (2)-(5), although only reactions (2) and (3) have originally been included in this model [29]. However, reactions (4) and (5) have been added to the H^+ model since H^0 atoms formed in (2) can react in these manners without an energy barrier [36,37,30,35], so that the probabilities for these reactions are great. It should be noted that neither the original H^+ model nor the H^+ model with reactions (4) and (5) added could fit the experimental results [17,18]. However, the H^+ model (i.e. reactions (2) and (3)) is foundation of all models proposed for LITB process so far. The main difference between these models is the origin of H^+ ions and the moment at which they reach the interface, but all models assume that interface traps are formed in reactions (2) and (3) [9,10,26]. In the case of normal interface trap buildup, for which the H^+ model was originally proposed [29,38,39], the H^+ ions arrive at the interface during time interval ranging from 1 to 10^4 s [40,38] after pulsed irradiation, which is much shorter than time interval in which LITB occurs (even up to 10^7 s [10,18]). According to recently proposed LITB process models [9,10], the H^+ ions are created in the cracking reaction of H_2

molecules in the oxide, after diffusion of H_2 from the structures adjacent to the gate oxide. The H^+ then drifts to the interface to take part in reactions (2) and (3). Finally, the latest model [26] for LITB process assumes the capture of radiation-induced H^+ ions at O vacancies and their release and drift towards the interface at later annealing times.

In the case of higher annealing temperatures (Fig. 3), the LITB process, which is in correlation with the latent ΔN_{ot} decrease, appears earlier, because of the faster diffusion of H_2 molecules from adjacent structures and earlier liberation of captured H^+ ions. The creation rate of interface traps, i.e. the slope of ΔN_{it} curve during the LITB process, increases with temperature, as a consequence of the dependence of reaction (1) on temperature (activation energy of this reaction is approximately 1 eV [11,18]). Also, in the case of higher temperature, the time to beginning of passivation process is shorter, because of the faster diffusion of H_2O molecules to the interface.

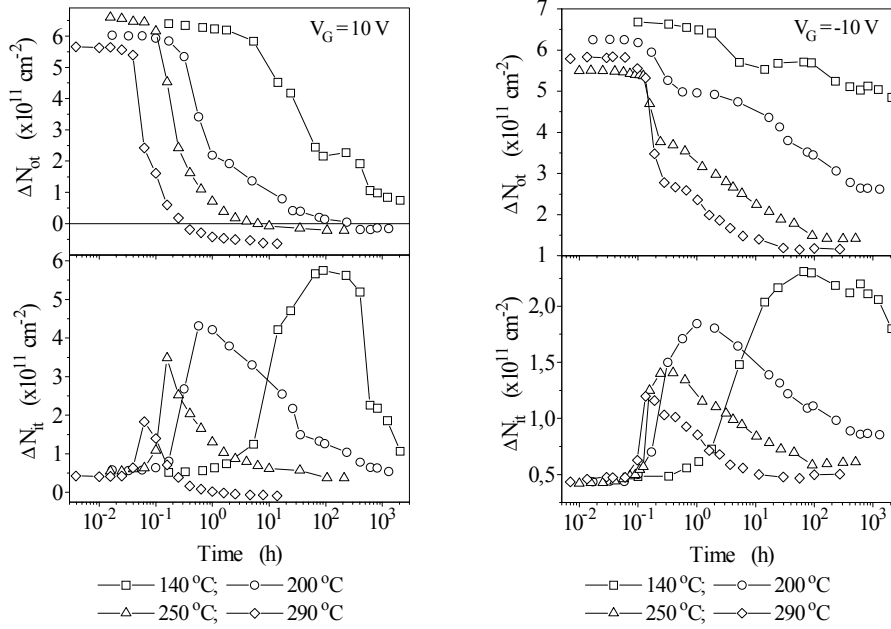
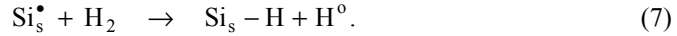


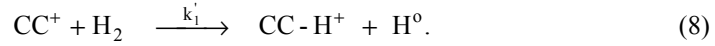
Fig. 3. ΔN_{ot} and ΔN_{it} during annealing with $V_G = 10$ V at different temperatures. Fig. 4. ΔN_{ot} and ΔN_{it} during annealing with $V_G = -10$ V at different temperatures.

It should be also noted that $\Delta N_{it,max}$ is lower in the case of a higher temperature. One of the reasons for such behaviour can be the existence of passivation reactions between H_2 molecules and interface traps above 200 °C [41]:



This reaction decreases the number of both the H_2 molecules, which diffuse towards bulk of the oxide, and interface traps. Other possibility is that the H_2O molecules, because of the faster diffusion, arrive at the interface earlier and contribute to the passivation process before significant density of interface traps is formed.

Figure 4 shows the changes in ΔN_{ot} and ΔN_{it} during annealing at various temperatures with $V_G = -10$ V. As can be seen, $\Delta N_{it,max}$, as well as the time to beginning of the LITB process depend on annealing temperature as in the case of $V_G = 10$ V, but the values of ΔN_{it} are considerably lower (see Fig. 3). The LITB process may seem unexpected, since oxide electric field is negative and H^+ ions are prevented to arrive at the interface. However, the explanation for such behaviour lies in a two-stage nature of the reaction (1) [11]. Namely, in the first stage H^o atom is created:



and the H^+ ion is a product of the second stage of this reaction (see Ref. [11]). Formed H^o atom can leave the place of creation and diffuse towards the interface to create the interface trap in reaction (3). The reasons for dependence of both the creation rate of ΔN_{it} and values of $\Delta N_{it,max}$ on temperature are the same as at $V_G = 10$ V.

4.1 Numerical simulation

Besides the above qualitative analysis of the behaviour of interface traps, the numerical modeling of their kinetics can be performed. Namely, on the basis of bimolecular theory [42] and reactions (1)-(6), the following differential equations are obtained for the H-W model:

$$\frac{d[H^+]}{dt} = k_1[CC^+][H_2] - k_2[H^+][e^-], \quad (9)$$

$$\frac{d[Si_s^*]}{dt} = k_3[Si_sH][H^o] - k_4[Si_s^*][H^o] - k_6[Si_s^*][H_2O], \quad (10)$$

$$\frac{d[H^o]}{dt} = k_2[H^+][e^-] - (k_3/t_{ox})[Si_sH][H^o] - (k_4/t_{ox})[Si_s^*][H^o] - k_5[H^o]^2 + (k_6/t_{ox})[Si_s^*][H_2O], \quad (11)$$

$$\frac{d[H_2]}{dt} = -k_1[CC^+][H_2] + (k_3/t_{ox})[Si_sH][H^o] + k_5[H^o]^2, \quad (12)$$

$$\frac{d[Si_sH]}{dt} = -k_3[Si_sH][H^o] + k_4[Si_s^*][H^o], \quad (13)$$

$$\frac{d[CC^+]}{dt} = -k_1[CC^+][H_2], \quad (14)$$

$$\frac{d[e^-]}{dt} = 0. \quad (15)$$

Reactions (9)-(15) describe the kinetics of interface traps in irradiated transistors during annealing with positive gate bias. The numerical fourth-order Runge-Kutta method with adaptive step-size [43] was used to solve this system of coupled differential equations. The set of unknown reaction rate constants and starting values of unknown reagent concentrations was found as described in [17].

Figure 5 gives the results of numerical simulation for annealing with $V_G = 10$ V at

various temperatures. The parameters of simulation at 140 °C are: $[\text{Si}_s^\bullet]_0 \equiv \Delta N_{it}(0) = 4.5 \times 10^{10} \text{ cm}^{-2}$ ($\Delta N_{it}(0)$ is the interface trap density at the start of annealing), $[\text{H}^0]_0 = 10^{14} \text{ cm}^{-3}$, $[\text{H}_2]_0 = 0$, $[\text{CC}^+]_0 = 3.25 \times 10^{16} \text{ cm}^{-3}$, $[\text{Si}_s\text{H}]_0 = 5 \times 10^{12} \text{ cm}^{-2}$, $[\text{e}^-]_0 = 3.5 \times 10^{13} \text{ cm}^{-3}$, $k_1 = 10^{-15} \text{ cm}^3/\text{h}$, $k_2 = 2.4 \times 10^{-15} \text{ cm}^3/\text{h}$, $k_3 = 10^{-15} \text{ cm}^3/\text{h}$, $k_4 = 0.4 \times k_3$, $k_5 = 0.09 k_3$, $k_6 = 2 \times 10^{-16} \text{ cm}^3/\text{h}$, $k_7 = 10 \text{ cm}^3/\text{h}$, $n = 0.08$, $a = 8.5$. H_2 molecules, which are cracked at CC^+ centers, and H_2O molecules need some time to arrive to the interface: t_{lat} and t_{lat1} , respectively [18]. For this temperature: $t_{lat} = 0.15 \text{ h}$, and $t_{lat1} = 2 \text{ h}$, while the initial concentration of delayed H^+ ions which arrive at the interface is $c = 2.9 \times 10^{16} \text{ cm}^{-3}$.

Different parameters at 200 °C, than at 140 °C, are: $[\text{CC}^+]_0 = 2.5 \times 10^{16} \text{ cm}^{-3}$, $k_1 = 6.3 \times 10^{-14} \text{ cm}^3/\text{h}$, $k_2 = 2 \times 10^{-13} \text{ cm}^3/\text{h}$, $k_6 = 4.2 \times 10^{-14} \text{ cm}^3/\text{h}$, $n = 0.138$, $t_{lat} = 0.12 \text{ h}$, $t_{lat1} = 0.126 \text{ h}$, $c = 1.8 \times 10^{16} \text{ cm}^{-3}$, for 250 °C: $[\text{CC}^+]_0 = 2.1 \times 10^{16} \text{ cm}^{-3}$, $k_1 = 10^{-12} \text{ cm}^3/\text{h}$, $k_2 = 8 \times 10^{-13} \text{ cm}^3/\text{h}$, $k_6 = 1.5 \times 10^{-12} \text{ cm}^3/\text{h}$, $n = 0.21$, $a = 9.65$, $t_{lat} = 0.045 \text{ h}$, $t_{lat1} = 0.022 \text{ h}$, $c = 0.85 \times 10^{16} \text{ cm}^{-3}$ and for 290 °C: $[\text{CC}^+]_0 = 1.87 \times 10^{16} \text{ cm}^{-3}$, $k_1 = 6.1 \times 10^{-12} \text{ cm}^3/\text{h}$, $k_2 = 2 \times 10^{-12} \text{ cm}^3/\text{h}$, $k_6 = 1.5 \times 10^{-11} \text{ cm}^3/\text{h}$, $n = 0.074$, $a = 8.32$, $t_{lat} = 0.034 \text{ h}$, $t_{lat1} = 0.003 \text{ h}$, $c = 0.95 \times 10^{16} \text{ cm}^{-3}$.

On the basis of above presented results of numerical simulation, the activation energy for some reactions can be determined. Namely, using the Arrhenius equation:

$$k = k_0 \exp\left(-\frac{E_a}{k_B T}\right) \quad (16)$$

where k_B is the Boltzmann's constant, the values of the activation energies are obtained for reaction (1): $E_a = 1.17 \text{ eV}$ (this value is in good agreement with $E_a = 1 \text{ eV}$ [11] and $E_a = 1.1 \text{ eV}$ [18]); reaction (2): $E_a = 0.9 \text{ eV}$ and reaction (6): $E_a = 1.5 \text{ eV}$. Figure 6 shows the dependencies of natural logarithms of reaction rate constants k_1 , k_2 and k_6 on reciprocal temperature.

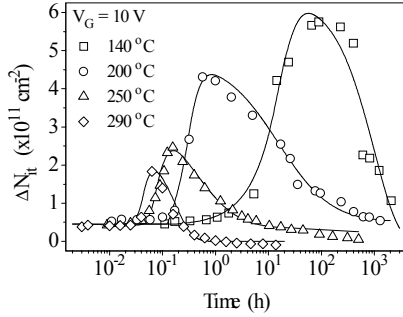


Fig. 5. ΔN_{it} during annealing with $V_G = 10 \text{ V}$ at different temperatures. The curves represent the results of numerical modeling based on the H-W model.

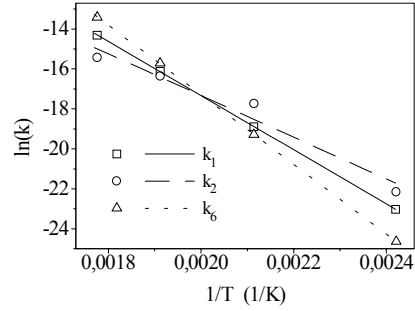


Fig. 6. Dependencies of reaction rate constants k_1 , k_2 and k_6 on reciprocal annealing temperature.

⁶ The relations between reaction rate constants k_3 , k_4 and k_5 are obtained on the basis of the radius captures of the reactants of corresponding reactions [44,18].

Figure 7 gives the results of numerical simulation for annealing with $V_G = -10$ V at various temperatures. The differential equations for modeling of annealing under negative bias are similar to the system (9)-(15). However, since the reaction (2) doesn't exist in the case of negative bias, it means that there are no equations (9) and (15). Also, k_1 should be substituted with k'_1 , and the term $k_2[H^+][e^-]$ in the equation (11) with the term $k'_1[CC^+][H_2]$.

Different parameters for annealing with $V_G = -10$ V than with $V_G = 10$ V, for $t = 140$ °C, are: $[CC^+]_0 = 1.85 \times 10^{16} \text{ cm}^{-3}$ for $t = 200$ °C: $[CC^+]_0 = 1.4 \times 10^{16} \text{ cm}^{-3}$, $k'_1 = 8 \times 10^{-15} \text{ cm}^3/\text{h}$, and for $t = 250$ °C: $[CC^+]_0 = 1.2 \times 10^{16} \text{ cm}^{-3}$, $k'_1 = 9 \times 10^{-16} \text{ cm}^3/\text{h}$, $k_6 = 1.6 \times 10^{-12} \text{ cm}^3/\text{h}$, $n = 0.175$, $a = 10$.

4.2 Charge pumping (CP) method

To check the above shown experimental results for ΔN_{it} , obtained by the MG method, the CP method was also used. Figure 8 shows ΔN_{it} during annealing at various temperatures with $V_G = 10$ V, obtained by CP method. The average interface trap densities are determined as $\Delta N_{it} = N_{it}(t) - N_{it0}$, where $N_{it}(t)$ is the absolute interface trap density after annealing time t , and N_{it0} is the absolute interface trap density before irradiation. These interface trap densities are determined in the following manner [22,23]:

$$N_{it} = D_{it} \times \Delta E = \frac{I_{cp,max}}{f q A_G} \quad (17)$$

where $D_{it}[\text{cm}^{-2}\text{eV}^{-1}]$ is the average energetic interface trap density, ΔE is the energetic range, $I_{cp,max}$ is the maximum value of the CP current, q is the absolute value of the electron charge, and $A_G = 6.163 \times 10^{-6} \text{ cm}^2 \times \text{cell number}$ [20] is area under the gate active in charge-pumping.

Figure 9 gives ΔN_{it} during annealing at 200 °C and $V_G = \pm 10$ V, obtained by MG and CP methods. On the basis of this figure, and the comparison between Figs. 3 and 8, it can be concluded that the qualitative behaviours of ΔN_{it} obtained by both methods are the same, but the values of ΔN_{it} are significantly lower in the case of CP method. This qualitative agreement between the experimental results obtained by MG and CP methods confirms our previous results [17,18], i.e. the existence of the LITB process and its dependence on temperature. The sources of quantitative differences in ΔN_{it} values may be different widths and/or positions of energetic range ΔE within silicon band gap, in which the interface traps are registered by CP and MG methods. In the case of CP method, we have determined the energetic range of $\Delta E = 0.466 \text{ eV}$ [45], centered around midgap.

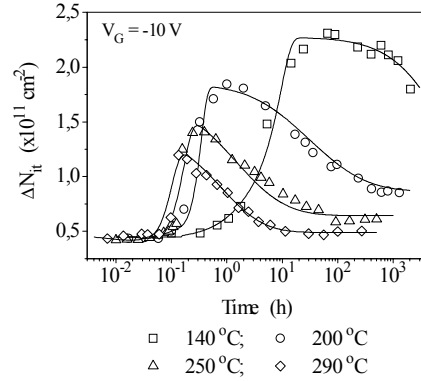


Fig. 7. ΔN_{it} during annealing with $V_G = -10$ V at different temperatures: The curves represent the results of numerical modeling based on the H-W model.

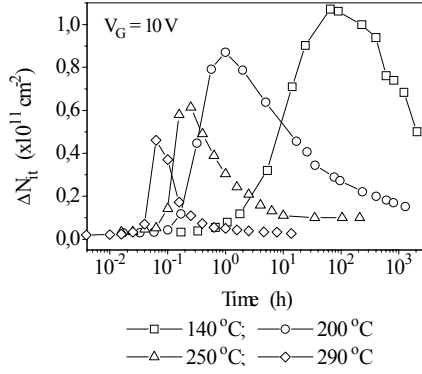


Fig. 8. ΔN_{it} during annealing with $V_G = 10$ V at different temperatures, obtained by CP method.

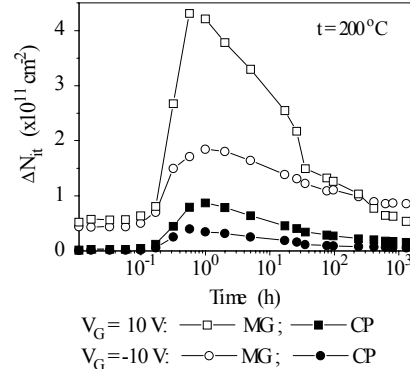


Fig. 9. ΔN_{it} during annealing at 200 °C and $V_G = \pm 10$ V, obtained by MG and CP methods.

In the case of MG method, the average density of interface traps is determined in the range from midgap, where surface potential is $\psi_s \equiv \psi_B = 0.381$ V,⁷ to the value of surface potential of $\psi_s \equiv \psi_T$, which corresponds to the threshold voltage V_T . Since for $V_G = V_T$ the surface potential has values between $\psi_{T1} = 2\psi_B$ and $\psi_{T2} = 2\psi_B + 6U_T$ ($U_T = k_B T/q = 0.02587$ V) [46], it can be concluded that energetic range ΔE has value between $\Delta E_1 = q(\psi_{T1} - \psi_B)$ and $\Delta E_2 = q(\psi_{T2} - \psi_B)$, i.e. 0.381-0.536 eV. For MG method, we have estimated the value of $\Delta E = 0.424$ eV [45], which is very close to the value obtained for CP method (0.466 eV). It means that the disagreement in values of ΔN_{it} obtained by these methods cannot be the consequence of difference in ΔE , but rather the consequence of different portions of band gap in which ΔN_{it} values are determined (i.e. positions of ΔE within band gap). Namely, since the distribution of interface traps within band gap of silicon is not uniform, but has the 'U'-shape [1], these portions within band gap are very important. The density of interface traps is greater at the band gap edges (accessible to MG method), and is lower around midgap (accessible to CP method).

It should be also noted that CP method gives ΔN_{it} predominantly for the $\text{SiO}_2/\text{n-epi}$ interface, while MG method senses interface traps at the channel interface (see the cross section of used transistors [19]), what can also contribute to observed quantitative disagreements [47]. Finally, owing to a great difference in the effective frequencies of two techniques, different amounts of 'border' traps contribute to signals measured by them, leading to an overestimation of the number of 'true' interface traps by the midgap method [48].

4.3 Activation energy of the LITB process

Activation energy E_a of the LITB process can be determined by Arrhenius equation:

⁷ $\psi_B = (kT/q) \ln(N_A/n_i)$, where N_A is the concentration of acceptor ingredient in semiconductor and n_i is the intrinsic concentration.

$$t = t_0 \exp\left(\frac{E_a}{k_B T}\right) \quad (18)$$

where t is the annealing time, and t_0 is normalizing constant. Figure 10 shows the dependence of time for half of latent ΔN_{it} increase ($t_{1/2}$) on reciprocal temperature ($1/T$) for four annealing temperatures (140, 200, 250 and 290 °C) for EFP8N15 type transistors and for two temperatures (room-temperature and 55 °C) for the similar EFL1N10 type transistors [18] ($V_G = 10$ V for all transistors during annealing). The fitting through all experimental values gives the activation energy of $E_{a1} = 0.63$ eV, and division to two temperature ranges: $E_{a2} = 0.54$ eV (room-temperature - 140 °C) and $E_{a3} = 0.47$ eV (200 - 290 °C). In this figure, it can be seen that more precise fitting is performed in the case of two temperature ranges. The obtained values of E_a are probably in relation with activation energy of diffusion of H_2 molecules ($E_a \approx 0.45$ eV). This is in agreement with the H-W model in which H_2 molecules diffusing from structures adjacent to gate oxide towards the interface, are responsible for the LITB process.

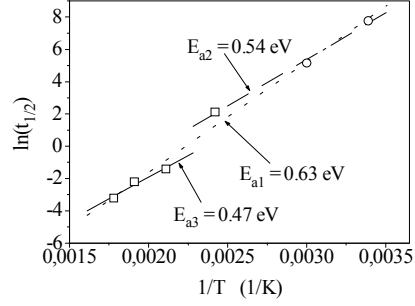


Fig. 10. Dependence of time for half of latent ΔN_{it} increase on reciprocal temperature.

4.4 Isochronal annealing experiments

ΔN_{ot} and ΔN_{it} obtained by MG and CP methods during isochronal annealing are presented in Fig. 11. The transistors were kept at each temperature for $\tau = 5$ min, the temperature interval between two annealing points was $\Delta t = 10$ °C, and gate bias was $V_G = 10$ V. As can be seen, the values of ΔN_{ot} and ΔN_{it} are almost constant up to temperature of 175 °C. After this temperature, the sudden increase of ΔN_{it} , accompanied by the sudden decrease of ΔN_{ot} , is observed. It is one more evidence that formation of interface traps is in correlation with the annealing of the oxide trapped charge. ΔN_{it} starts to decrease above 225 °C. As can also be seen, the qualitative behaviours of ΔN_{it} obtained by MG and CP methods are the same, but the values of ΔN_{it} are significantly lower in the case of CP method.

On the basis of data in Fig. 11, using the model proposed by Danchenko et al. [49], which has been widely used in the literature [50-52], the activation energy distribution of the annealing of oxide trapped charge was determined. Namely, using appropriate approximations, it can be shown [49] that the activation energy ε is given by the transcendental equation:

$$\frac{\varepsilon}{\eta} + \ln\left(\frac{\varepsilon}{\eta} + 2\right) = \ln(Ac\eta), \quad (19)$$

where $\eta = k_B T$, A is the constant called 'frequency factor', and $c = \tau/(k_B \Delta T)$ is the tempering constant. The initial distribution, i.e. distribution of oxide trapped charge

before annealing, in activation energies $n_o(\epsilon)$ is [49]:

$$n_o(\epsilon) = -\frac{dN}{d\eta} \frac{1}{\epsilon/\eta + 1}, \quad (20)$$

where N is unannealed fraction of oxide trapped charge, defined as [49,50]:

$$N(t) = \frac{\Delta N_{ot}(t)}{\Delta N_{ot}(0)}, \quad (21)$$

where $\Delta N_{ot}(0)$ is the oxide trapped charge density after irradiation (before annealing), and $\Delta N_{ot}(t)$ is this density at the moment t during annealing.

The procedure of finding of initial energy distribution $n_o(\epsilon)$ is the following. The values of activation energy for each temperature of isochronal annealing are found first by the transcendental equation (19) (in this paper, the iteration method was used to solve this equation [43]). After that, the values of $dN/d\eta = (1/k_B)dN/dT$ derivative are numerically determined [43] on the basis of the dependence of unannealed fraction N on η , i.e. on T (N has the same shape as ΔN_{ot} , shown in Fig. 11).

Figure 12 presents the initial distribution of oxide trapped charge in activation energies $n_o(\epsilon)$ for three values of the frequency factor A . It can be concluded that the majority of oxide trapped charge has the same value of activation energy (sharp peaks in Fig. 12). However, distribution $n_o(\epsilon)$ is very sensitive to the value of constant A , so that one should be very cautious when discussing E_a values obtained by Danchenko's method. The obtained energy distributions are even qualitatively different from those found from TSC measurements by Fleetwood et al. [53] in a wide range of oxides.

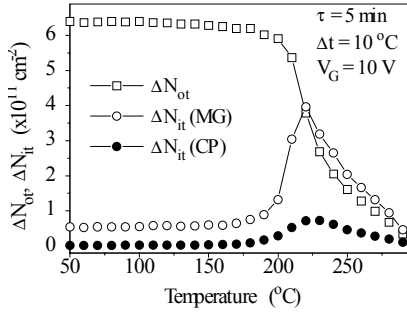


Fig. 11. ΔN_{it} and ΔN_{ot} during isochronal annealing.

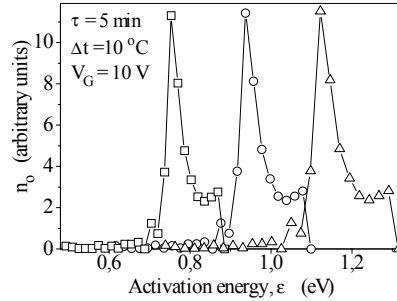


Fig. 12. Distributions of oxide trapped charge for three values of frequency factor A : 10^5 , 10^7 and 10^9 s^{-1} , respectively.

5. CONCLUSIONS

The LITB process has been observed in the wide range of temperatures during annealing of gamma-ray irradiated n-channel power VDMOS transistors. The experimental results are in consistence with the H-W model. The numerical simulation of

the LITB process, based on the H-W model, has been successfully performed. The MG and CP methods have been used for determination of interface trap densities, and have yielded qualitatively similar results. Observed quantitative differences have been discussed. On the basis of isothermal annealing, the activation energy of the LITB process has been determined, showing that H₂ molecules are probably responsible for this process. The experimental results of isochronal annealing have confirmed that the increase in ΔN_{it} is in correlation with the decrease in ΔN_{ot} . Application of Danchenko's model combined with electrical measurement technique for determination of oxide trap charge energy distribution has been critically discussed.

REFERENCES

1. T.P. Ma and P.V. Dressendorfer, *Ionizing radiation effects in MOS devices and circuits*, Wiley, New York, 1989.
2. A.G. Holmes-Siedle, "The space charge dosimeter-General principles of a new method of radiation dosimetry", *Nuclear Instruments and Methods*, **121**, 169-179 (1974).
3. A. Kelleher, M. O'Sullivan, J. Ryan, B. O'Neal, and W. Lane, Development of the radiation sensitivity of PMOS dosimeters, *IEEE Trans. Nuclear Science*, **NS-39** (3), 342-346 (1992).
4. G. Ristić, S. Golubović, and M. Pejović, pMOS transistors for dosimetric application, *Electronics Letters*, **29** (18), 1644-1646 (1993).
5. G. Ristić, S. Golubović, and M. Pejović, P-channel metal-oxide-semiconductor dosimeter fading dependencies on gate bias and oxide thickness, *Applied Physics Letters*, **66** (1), 88-89 (1995).
6. G. Ristić, S. Golubović, and M. Pejović, Sensitivity and fading of pMOS dosimeters with thick gate oxide, *Sensors and Actuators A. Physical*, **A 51**, 153-158 (1996).
7. G. Ristić, A. Jakšić, and M. Pejović, pMOS dosimetric transistors with two-layer gate oxide, *Sensors and Actuators A. Physical*, **A 63**, 129-134 (1997).
8. J.R. Schwank, D.M. Fleetwood, M.R. Shaneyfelt, and P.S. Winokur, Latent thermally activated interface-trap generation in MOS devices, *IEEE Electron Devices Letters*, **13** (4), 203-205 (1992).
9. J.R. Schwank, D.M. Fleetwood, M.R. Shaneyfelt, P.S. Winokur, C.L. Axness, and L.C. Riewe, Latent interface-trap buildup and its implications for hardness assurance, *IEEE Trans. Nuclear Science*, **NS-39** (6), 1953-1963 (1992).
10. D.M. Fleetwood, W.L. Warren, J.R. Schwank, P.S. Winokur, M.R. Shaneyfelt, and L.C. Riewe, Effects of interface traps and border traps on MOS postirradiation annealing response, *IEEE Trans. Nuclear Science*, **NS-42** (6), 1698-1707 (1995).
11. R.E. Stahlbush, A.H. Edwards, D.L. Griscom, and B.J. Mrstik, Post-irradiation cracking of H₂ and formation of interface states in irradiated metal-oxide-semiconductor field-effect transistors, *Journal of Applied Physics*, **73** (2), 658-667 (1993).
12. R.E. Stahlbush and A.H. Edwards, Effects of introducing H₂ into irradiated MOSFETs from room temperature to 250 °C, *The Physics and Chemistry of SiO₂ and the Si-SiO₂ Interface*, C.R. Helms and B.E. Deal, eds., Plenum Press, New York, 1993, pp. 489-498.
13. J.F. Conley Jr. and P.M. Lenahan, Room temperature reactions involving silicon dangling bond centers and molecular hydrogen in amorphous SiO₂ thin films on silicon, *Applied Physics Letters*, **62** (1), 40-42 (1993).
14. J.F. Conley Jr. and P.M. Lenahan, Electron spin resonance analysis of EP center interactions with H₂: Evidence for a localized EP center structure, *IEEE Trans. Nuclear Science*, **NS-42** (6), 1740-1743 (1995).
15. M. Pejović, G. Ristić, and A. Jakšić, Formation and passivation of interface traps in irradiated n-channel power VDMOSFETs during thermal annealing, *Applied Surface Science*, **108**, 141-148, 1997.
16. M. Pejović and G. Ristić, Creation and passivation of interface traps in irradiated MOS transistors during annealing at different temperatures, *Solid-State Electronics*, **41** (5), 715-720 (1997).
17. G.S. Ristić, M.M. Pejović, and A.B. Jakšić, Numerical simulation of creation-passivation kinetics of interface traps in irradiated n-channel power VDMOSFETs during thermal annealing with various gate biases, *Microelectronic Engineering*, **40**, 51-60 (1998).

18. G.S. Ristić, M.M. Pejović, and A.B. Jakšić, Modelling of kinetics of creation and passivation of interface traps in metal-oxide-semiconductor transistors during postirradiation annealing, *Journal of Applied Physics*, **83** (6), 2994-3000 (1998).
19. A. Jakšić, M. Pejović, G. Ristić, and S. Raković, Latent interface-trap generation in commercial power VDMOSFETs, *IEEE Trans. Nuclear Science*, **45** (3), 1365-1371 (1998).
20. P. Habaš, Z. Prijjić, D. Pantić, and N.D. Stojadinović, Charge-pumping characterization of SiO₂/Si interface in virgin and irradiated power VDMOSFETs, *IEEE Trans. Electron Devices*, **ED-43** (12), 2197-2209 (1996).
21. P.J. McWhorter and P.S. Winokur, Simple technique for separating the effects of interface traps and trapped-oxide charge in metal-oxide-semiconductor transistors, *Applied Physics Letters*, **48** (1), 133-1135 (1986).
22. A.B. M. Elliot, The use of charge pumping currents to measure surface state densities in MOS transistors, *Solid-State Electronics*, **19**, 241-247 (1976).
23. G. Groeseneken, H.E. Maes, N. Beltran, and R.F. De Keersmaecker, A reliable approach to charge-pumping measurements in MOS transistors, *IEEE Trans. Electron Devices*, **ED-31** (1), 42-53 (1984).
24. N.S. Saks, R.B. Klein, R.E. Stahlbush, B.J. Mrstik, and R.W. Rendell, Effects of post-stress hydrogen annealing on MOS oxides after Co-60 irradiation or Fowler-Nordheim injection, *IEEE Trans. Nuclear Science*, **NS-40** (6), 1341 (1993).
25. A.D. Marwick and D.R. Young, Measurements of hydrogen in metal-oxide-semiconductor structures using nuclear reaction profiling, *Journal of Applied Physics*, **63** (7), 2291-2298 (1988).
26. M.J. Johnson and D.M. Fleetwood, Correlation between latent interface trap buildup and 1/f noise in metal-oxide-semiconductor transistors, *Applied Physics Letters*, **70** (9), 1158-1160 (1997).
27. P.M. Lenahan and P.V. Dressendorfer, Hole traps and trivalent silicon centers in metal/oxide/silicon devices, *Journal of Applied Physics*, **55** (10), 3495-3499 (1984).
28. Y.Y. Kim and P.M. Lenahan, Electron-spin-resonance study of radiation-induced paramagnetic defects in oxides grown on (100) silicon substrates, *Journal of Applied Physics*, **64** (7), 3551-3557 (1988).
29. D.L. Griscom, D.B. Brown, and N.S. Saks, Nature of radiation-induced point defects in amorphous SiO₂ and their role in SiO₂-on-Si structures, *The Physics and Chemistry of SiO₂ and the Si-SiO₂ Interface*, C.R. Helms and B.E. Deal, eds., Plenum Press, New York, 1988, pp. 287-298.
30. K.L. Brower and S.M. Myers, Chemical kinetics of hydrogen and (111) Si-SiO₂ interface defects, *Applied Physics Letters*, **57** (2), 162-164 (1990).
31. J.H. Stathis and E. Cartier, Atomic hydrogen reactions with P_b centers at the (100) Si-SiO₂ interface, *Physical Review Letters*, **72** (17), 2745-2748 (1994).
32. G.J. Gerardi, E.H. Poindexter, and P.J. Caplan, Interface traps and P_b centers in oxidized (100) silicon wafers, *Applied Physics Letters*, **49** (6), 348-350 (1986).
33. E.H. Poindexter, Chemical reactions of hydrogenous species in the Si-SiO₂ system, *Journal of Non-Crystalline Solids*, **187**, 257-263 (1995).
34. J.H. Stathis and L. Dori, Fundamental chemical differences among P_b defects on (111) and (100) silicon, *Applied Physics Letters*, **58** (15), 1641-1643 (1991).
35. E. Cartier, J.H. Stathis, and D.A. Buchanan, Passivation and depassivation of silicon dangling bonds at the Si/SiO₂ interface by atomic hydrogen, *Applied Physics Letters*, **63** (11), 1510-1512 (1993).
36. D.L. Griscom, Diffusion of radiolytic molecular hydrogen as a mechanism for the post-irradiation buildup of interface states in SiO₂-on-Si structures, *Journal of Applied Physics*, **58** (7), 2524-2533 (1985).
37. M.L. Reed and J.D. Plummer, Si-SiO₂ interface trap production by low-temperature thermal processing, *Applied Physics Letters*, **51** (7), 514-516 (1987).
38. N.S. Saks, C.M. Dozier, and D.B. Brown, Time dependence of interface trap formation in MOSFETs following pulsed irradiation, *IEEE Trans. Nuclear Science*, **NS-35** (6), 1168-1177 (1988).
39. N.S. Saks and D.B. Brown, Interface trap formation via the two-stage H⁺ process, *IEEE Trans. Nuclear Science*, **NS-36** (6), 1848-1857 (1989).
40. F.B. McLean, A framework for understanding radiation-induced interface states in SiO₂ MOS structures, *IEEE Trans. Nuclear Science*, **NS-27** (6), 1651-1657 (1980).
41. K.L. Brower, Passivation of paramagnetic Si-SiO₂ interface states with molecular hydrogen, *Applied Physics Letters*, **53** (6), 508-510 (1988).
42. M.L. Reed and J.D. Plummer, Chemistry of Si-SiO₂ interface trap annealing, *Journal of Applied Physics*, **63** (12), 5776-5793 (1988).
43. W.H. Press, B.P. Flannery, S.A. Teukolsky, and W.T. Vetterling, *Numerical recipes*, Cambridge

- University Press, Cambridge, 1986.
44. M.L. Reed, *Si-SiO₂ interface trap anneal kinetics*, PhD Thesis, Stanford University, Stanford, 1987.
 45. G.S. Ristić, *Radiation and postirradiation effects on power VDMOS transistors and PMOS dosimetric transistors* (in Serbian), PhD Thesis, Faculty of Electronic Engineering, University of Niš, 1998.
 46. S.M. Sze, *Physics of semiconductor devices*, Wiley, New York, 1981.
 47. A. Jak{i} and P. Igi}, Use of charge pumping for characterising interface traps during thermal annealing of irradiated power VDMOSFETs, *Electronics Letters*, **32** (23), 2183-2184, 1996.
 48. J.R. Schwank, D.M. Fleetwood, M.R. Shaneyfelt, and P.S. Winokur, A critical comparison of charge-pumping, dual-transistor, and midgap measurement techniques, *IEEE Trans. Nuclear Science*, **NS-40** (6), 1666-1677 (1993).
 49. V. Danchenko, U.D. Desai, and S.S. Brashears, Characteristics of thermal annealing of radiation damage in MOSFETs, *Journal of Applied Physics*, **39** (5), 2417-2424 (1968).
 50. A. Mallik, J. Vasi, and A.N. Chandorkar, The nature of the hole traps in reoxidized nitrated oxide gate dielectrics, *Journal of Applied Physics*, **74** (4), 2665-2668 (1993).
 51. L. Dusseau, T.L. Randolph, R.D. Schrimpf, K.F. Galloway, F. Saigne, J. Fesquet, J. Gasiot, and R. Ecoffet, Prediction of low dose-rate effects in power metal oxide semiconductor field effect transistors based on isochronal annealing measurements, *Journal of Applied Physics*, **81** (5), 2437-2441 (1997).
 52. F. Saigne, L. Dusseau, L. Albert, J. Fesquet, J. Gasiot, J. P. David, R. Ecoffet, R.D. Schrimpf, and K.F. Galloway, Experimental determination of the frequency factor of thermal annealing processes in metal-oxide semiconductor gate-oxide structures, *Journal of Applied Physics*, **82** (8), 4102-4107 (1997).
 53. D.M. Fleetwood, Border traps in MOS devices, *IEEE Trans. Nuclear Science*, **NS-39** (2), 269-271, 1992.

IZOTERMALNO I IZOHRONALNO ODŽARIVANJE n-KANALNIH VDMOS TRANZISTORA SNAGE OZRAČENIH GAMA-ZRAČENJEM

Goran S. Ristić, Momčilo M. Pejović, Aleksandar B. Jakšić

Ispitivano je ponašanje gustina zahvaćenog naelektrisanja i površinskih stanja kod ozračenih n-kanalnih VDMOS tranzistora snage tokom njihovog izotermalnog i izohronalnog odžarivanja. Eksperimentalni rezultati su potvrdili postojanje procesa latentnog formiranja površinskih stanja (LITB proces). Izvršeno je uspešno numeričko modelovanje ovog procesa zasnovano na H-W modelu. Gustine površinskih stanja su određivane pomoću midgap i charge-pumping metode, i pokazano je dobro kvalitativno slaganje vrednosti dobijenih ovim metodama.

Ključne reči: površinska stanja, zahvaćeno naelektrisanje u oksidu, ozračivanje, odžarivanje, MOS tranzistor